Molecular Structures and Catalytical Performance in Suzuki-coupling Reaction of Novel Dipalladium Clip-shaped Complexes with Bifunctional Pyrazolate Ligands①

HU Xiao-Peng WANG Zhi-Feng
DENG Wei TONG Jin YU Shu-Yan②

(*Laboratory for Self-assembly Chemistry, Center of Excellence for Environmental Safety and Biological Effects, Beijing Key Laboratory for Green Catalysis and Separation, Department of Environment and Life, Beijing University of Technology, Beijing* 100124, *China*)

ABSTRACT A series of clip-shaped cationic molecular corners C1~C4 (C1 = $[(bpy)_2Pd_2(L^1)_2]^{2+}$, C2 = $[(dmbpy)_2Pd_2(L^1)_2]^{2+}$, C3 = $(bpy)_2Pd_2(L^2)_2]^{2+}$, C4 = $(dmbpy)_2Pd_2(L^2)_2]^{2+}$, bpy = 2,2-bipyridine, dmbpy = 4,4′-dimethyl-2,2-bipyridine) were synthesized through dipalladium complexes $[(bpy)_2Pd_2(NO_3)_2](NO_3)_2$, $[(dmbpy)_2Pd_2(NO_3)_2](NO_3)_2$ and bifunctional pyrazole ligands 4-(3,4-dimethoxyphenyl)-3,5-dimethyl-1H-pyrazol (HL^1) and 4,4′-(5-(1H-pyrazol-4-yl)-1,3-phenylene)dipyridine (HL^2). Complexes C1~C4 were characterized by ^1H and ^{13}C NMR, electrospray ionization mass spectrometry (ESI-MS), elemental analysis, and IR spectroscopy. The X-ray diffraction analysis of $C1{\cdot}2NO_3^-$ revealed a Pd_2 dimetallic clip-shaped structure which was synthesized by two bifunctional ligands doubly bridged by the $[(bpy)Pd]_2$ dimetal units. Additionally, all of the complexes with NO_3^- as counter anions exhibited high-efficiency catalytical performance in the Suzuki-coupling reaction attributed to the tunable impact and weak dinuclear Pd(II) ··Pd(II) intramolecular bonding interaction.

Keywords: **dipalladium supra molecules**, **bifunctional pyrazolate ligands**, **catalysis**, **Suzuki-coupling reaction;**
DOI: 10.14102/j.cnki.0254–5861.2011–3174

1 INTRODUCTION

Supramolecular chemistry has attracted significant research attention due to its rapid expansion to chemical sensors, host-guest interactions, catalysis and functional materials[1-5]. Coordination-driven self-assembly as a high efficient approach for the construction of molecular systems capable of well-defined molecular-level motion has become a field of growing interest and an important issue in this field as regards the metal-based molecular corners and tweezes, which display fascinating properties and applications such as catalysis, redox and photoluminescence[6-8]. Therefore, considerable efforts been have devoted to the design and synthesis of functional molecular corners with arms or tips for host-guest recognition, molecule separation and purification using various supramolecular interactions including hydrogen bonding, metal coordination, metal-metal bonding, hydrophobic forces, van der Waals forces, electrostatic efforts and π-π interactions[10-12]. Moreover, multimetallic catalysts in which multimetal centers are present in close proximity to each other exhibit better reactivity than equivalent mixtures of monometallic complexes[13-15]. To date, various organic ligands including pyridine-carboxylates, pyridine-phosphates, imidazole-carboxylates and amino acids containing O and N donors have been selected to construct multimetallic complexes with interesting structures and physical chemical properties[16-18]. However, it is still a challenge to rationally design and control the synthesis of multimetallic coordination polymers by choosing suitable organic ligands.

Pyrazole has the virtue of coordinating with metal ions by monodentate and bidentate and assembled through intermolecular hydrogen-bonding interaction[19, 20]. The coor-

Received 11 March 2011; accepted 27 May 2021 (**CCDC 2061870**)

① This work was supported by the Beijing Natural Science Foundation of China (2212002), National Natural Science Foundation of China (21906002, 21471011), the Beijing Municipal Science and Technology Project (KM202010005010), the Beijing Municipal High Level Innovative Team Building Program (IDHT20180504) and the Beijing Outstanding Young Scientist Program (BJJWZYJH01201910005017)

② Corresponding author. E-mail: selfassembly@bjut.edu.cn

dination chemistry of pyrazoles and its derivatives received particular attention not only for their beautiful and diverse structures like metal-based polymers, metallo-macrocycles, metallo-cages and so on, but also the broad application prospects and relevance in multimetal-centered catalysis, multielectron-transfer reaction and photophysical studies[21-23]. In the past few years, considerable attention has been paid to functional metal-organic assemblies that show promise in catalysis with environment-friendly[24] properties. Especially, palladium complexes were employed in the Suzuki-couping reaction for their high stability and remarkable efficiency. In our previous work, we have developed a series of novel homometallic/heterometallic supramolecular catalysts containing functional pyrazole ligands through self-assembly[25, 26]. Inspired by such work, we focus on the construction of supramolecules from functional pyrazolate ligands with dipalladium clips.

In this work, we successfully synthesized a series of functional clip-shaped supramolecular corners C1~C4 by using a novel kind of bifunctional pyrazolate ligands 4-(3,4-dimethoxyphenyl)-3,5-dimethyl-1H-pyrazol (HL[1]) and 4,4′-(5-(1H-pyrazol-4-yl)-1,3-phenylene)dipyridine (HL[2]) with dimetal motifs $[(bpy)_2Pd_2(NO_3)_2](NO_3)_2$ and $[(dmbpy)_2Pd_2(NO_3)_2](NO_3)_2$, as shown in Scheme 1. In addition, the supramolecular assemblies have been studied by ^{1}H and ^{13}C NMR, IR spectroscopy, electrospray ionization mass spectrometry (ESI-MS) and elemental analysis. Furthermore, we find that $C1{\cdot}2NO_3^-$, $C2{\cdot}2NO_3^-$, $C3{\cdot}2NO_3^-$ and $C4{\cdot}2NO_3^-$ showed good catalytic effect on the Suzuki-coupling reaction which are attributed to the tunable impact and weak Pd(II)··Pd(II) intramolecular bonding interaction.

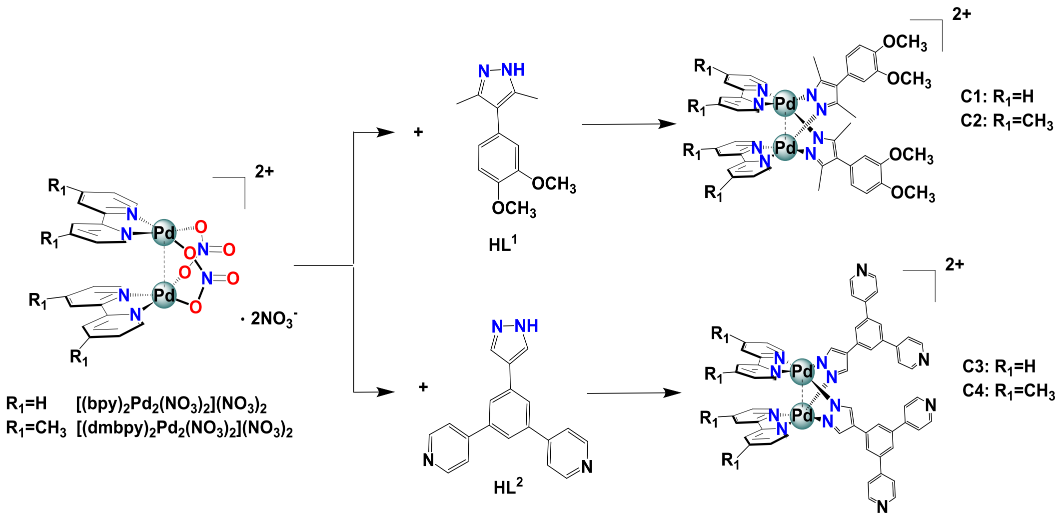

Scheme 1. Self-assembly of dipalladium corners C1-C4·$2NO_3^-$

2 EXPERIMENTAL

2. 1 Materials and methods

The FT-IR spectra were recorded as KBr pellets on a Shimadzu IR Prestige-21 spectrometer. NMR spectra of all compounds were recorded at 400 MHz on a Bruker AIVEN400 spectrometer. ESI-MS measurements were performed with a JEOL Accu-TOF-4G LC-plus mass spectrometer. The elemental analysis was performed on a Thermo Electron SPA Flash EA1112 analyzer.

2. 2 Synthesis of the ligands

The ligand HL[1] was synthesized as described in Scheme 2 by using similar methods in our group[19, 22] (See SI for the synthesis). ^{1}H NMR (400 MHz, DMSO): 12.24 (s, 1H, Pz*H*), 6.98 (d, *J* = 8 Hz, 1H, Ph*H*), 6.82 (d, *J* = 2 Hz, 1H, Ph*H*), 6.78 (m, 1H, Ph*H*), 3.76 (s, 6H, OCH_3), 2.17 (s, 6H, CH_3) ppm. ^{13}C NMR (400 MHz, DMSO): 149.00 (s, *3*-C_6H_3C), 147.44 (s, *4*-C_6H_3C), 145.34 (s, *2*-C_3HC), 135.79 (s, *4*-C_3HC), 127.09 (s, *1*-C_6H_3C), 121.35 (s, *3*-C_3HC), 117.32 (s, *6*-C_6H_3C), 113.18 (s, *2*-C_6H_3C), 112.42 (s, *5*-C_6H_3C), 55.92 (s, CH_3C), 55.91 (s, CH_3C), 13.32 (s, *5*-OCH_3C), 10.48 (s, *6*-OCH_3C) ppm.

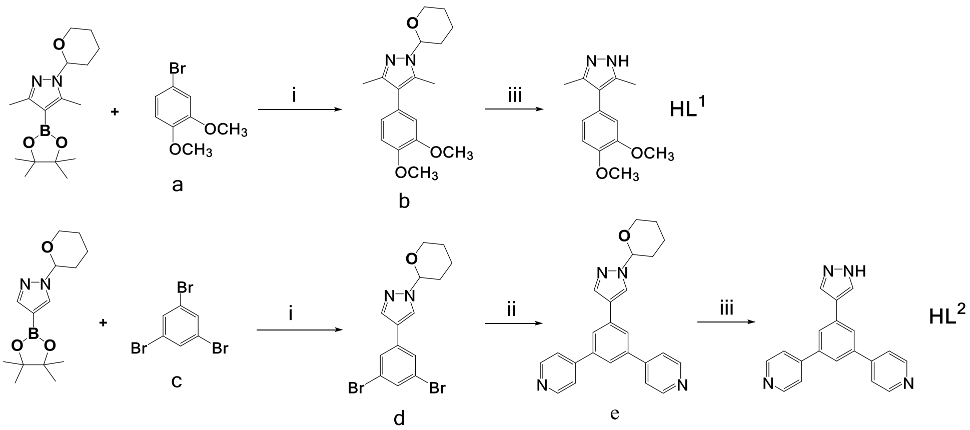

Scheme 2. Synthesis of HL^1 and HL^2: i. K_2CO_3, $Pd(PPh_3)_4$, reflux; ii. Pyb, K_2CO_3, $Pd(PPh_3)_4$, reflux; iii. HCl, methanol, reflux

The ligand HL^2 was synthesized by using similar methods in our group[25] (See SI for the synthesis). 1H NMR (400 MHz, DMSO): 13.05 (s, 1H, Pz*H*), 8.70 (d, *J* = 6 Hz, 4H, Bd*H*), 8.35 (s, 2H, Pz*H*), 8.13 (d, *J* = 1.6 Hz, 2H, Ph*H*), 7.99 (s, 1H, Ph*H*), 7.93 (d, *J* = 1.2 Hz, 4H, Bd*H*); ^{13}C NMR (400 MHz, DMSO): 150.65 (s, *2*-C_5H_4NC), 147.14 (s, *4*-C_5H_4NC), 139.20 (s, *3*-C_6H_3C), 135.40 (s, *1*-C_6H_3C), 133.41 (s, *2*-$C_3H_2N_2C$), 124.59 (s, *2*-C_6H_3C), 123.19 (s, *4*-C_6H_3C), 122.12 (s, *3*-$C_3H_2N_2C$), 120.95 (s, *3*-C_5H_4NC).

2. 3 Synthesis and characterization of clip-shaped supramolecular corners

The self-assembly of metallo-clip complex C1·$2NO_3^-$ is shown in Scheme 1. HL^1 (20.4 mg, 0.1 mmol) was added to a suspension solution of $[(bpy)_2Pd_2(NO_3)_2](NO_3)_2$ (38.6 mg, 0.05 mmol) in H_2O/actone (3:4 mL). The mixture was stirred for 2 h at room temperature, then moved to 80 °C for another 6 h. A ten-fold excess of KPF_6 was added to the solution which resulted in an immediate deposition. The mixture was continued stirring for 6 h, then the precipitation was filtered, washed with minimum amount of cold water and dried in vacuum to give yellow solid. The PF_6^- salt of C1 was obtained as yellow needle powders in quantitative yield (92%). C1·$2NO_3^-$: ^1H NMR (400 MHz, D_2O): 8.59 (d, 2H, *J* = 7.8 Hz, bpy*H*), 8.41 (d, 2H, *J* = 8.9 Hz, bpy*H*), 8.36 (t, 2H, *J* = 6.1 Hz, bpy*H*), 7.81 (t, 2H, *J* = 9.4 Hz, bpy*H*), 7.04 (d, 1H, *J* = 8.3 Hz, Ph*H*), 6.98 (s, 1H, Ph*H*), 6.94 (d, 1H, *J* = 8.2 Hz, Ph*H*), 3.87 (s, 5.2H, *J* = 2.9 Hz, OCH_3), 3.36 (s, 0.7H, OCH_3), 2.52 (s, 5H, CH_3), 2.33 (s, 1H, CH_3); ^{13}C NMR (400 MHz, MeOD): 156.91 (s, *2*-C_5H_4C), 150.75 (s, *3*-C_6H_3C), 149.00 (s, *4*-C_6H_3C), 148.08 (s, *6*-C_5H_4C), 147.40 (s, *2*-C_3HC), 142.00 (s, *4*-C_5H_4C), 127.90 (s, *1*-C_6H_3C), 125.88 (s, *3*-C_3HC), 123.97 (s, *3*-C_5H_4C), 121.96 (s, *6*-C_6H_3C), 121.73 (s, *2*-C_6H_3C), 113.20 (s, *5*-C_5H_4C), 111.69 (s, *5*-C_6H_3C), 55.27 (s, *3*-$C_5H_4OCH_3C$), 55.11 (s, *4*-$C_5H_4OCH_3C$), 12.24 (s, *4*-C_3HCH_3C), 11.62 (s, *5*-C_3HCH_3C). FT-IR (KBr, cm^{-1}): 3451(s), 2998(vs), 1613(s), 1506(s), 1434(s), 1351(w), 1231(vs), 1159(m), 1016(m), 742(w), 634(s). ESI-MS (CH_3CN, m/z): 493.1, 1132.2 for $[C1]^{2+}$, $[C1·PF_6^-]^+$. Anal. Calcd. (%) for $C_{46}H_{46}N_{10}O_{10}Pd_2$: C, 49.70; H, 4.17; N, 12.60. Found (%): C, 49.72; H, 4.16; N, 12.64.

The other three similar complexes C2, C3 and C4 are obtained by using the same method (See SI for the synthesis).

2. 4 X-ray structure determination

A light yellow block single crystal was selected for single-crystal X-ray diffraction analysis. Data collections were performed with an ω scan mode at 296(2) K in the range of $2.4<\theta<24.3°$ on a Bruker SMART APEX-II CCD diffractometer equipped with Mo*Kα* radiation (λ = 0.71073 Å). The crystal structure was solved by direct methods and refined by full-matrix least-squares method on F^2 by means of SHELXL software package[27, 28]. All non-hydrogen atoms were refined anisotropically and all hydrogen atoms were located and refined geometrically. Furthermore, calculations of distances and angles between some atoms were performed by DIAMOND or SHELXL. The final selected bond lengths and bond angles for C1·$2NO_3^-$ are listed in Table 1.

Crystal data for $C_{46}H_{46}N_{10}O_{10}Pd_2$ (M_r = 1111.73 g/mol): monoclinic system, space group $P2_1/c$, a = 22.2285(13), b = 12.4362(7), c = 16.9118(8) Å, β = 97.450(5)°, V = 4635.6(4) $Å^3$, Z = 4, T = 296(2) K, D_c = 1.593 g/cm^3, 11130 reflections measured (R_{int} = 0.0457, R_{sigma} = 0.0740) which were used in all calculations. The final R = 0.0527 ($I > 2\sigma(I)$) and wR = 0.1112 (all data).

Table 1. Selected Bond Lengths (Å), Bond Angles (°) and Hydrogen Bond Lengths (Å)

Bond	Dist.	Bond	Dist.	Bond	Dist.
Pd(1)–Pd(2)	3.0700(5)	Pd(1)–N(2)	1.998(3)	Pd(1)–N(4)	2.004(4)
Pd(1)–N(5)	2.018(4)	Pd(1)–N(6)	2.001(3)	Pd(2)–N(1)	2.013(4)
Pd(2)–N(3)	2.004(4)	Pd(2)–N(7)	2.018(4)		
Angle	(°)	Angle	(°)	Angle	(°)
N(1)–Pd(1)–Pd(2)	64.06(11)	N(2)–Pd(1)–N(4)	87.47(15)	N(7)–Pd(2)–N(8)	80.97(15)
N(8)–Pd(2)–Pd(1)	107.23(11)	N(2)–Pd(1)–N(5)	95.23(15)	N(2)–N(1)–Pd(2)	112.4(3)
N(2)–Pd(1)–N(6)	175.96(15)	C(2)–N(1)–Pd(2)	139.8(3)	N(4)–Pd(1)–Pd(2)	64.53(11)
N(1)–N(2)–Pd(1)	117.5(3)	N(4)–Pd(1)–N(5)	176.88(15)	C(4)–N(2)–Pd(1)	133.4(3)
N(5)–Pd(1)–Pd(2)	115.29(11)	N(4)–N(3)–Pd(2)	114.6(3)	N(6)–Pd(1)–N(4)	96.35(15)
N(6)–Pd(1)–Pd(2)	116.46(11)	C(17)–N(3)–Pd(2)	136.6(3)	N(6)–Pd(1)–N(5)	80.92(15)
N(1)–Pd(2)–Pd(1)	65.84(10)	N(3)–N(4)–Pd(1)	115.8(3)	C(37)–N(5)–Pd(1)	125.6(3)
N(1)–Pd(2)–N(7)	96.19(15)	C(15)–N(4)–Pd(1)	135.6(3)	C(41)–N(5)–Pd(1)	114.1(3)
N(1)–Pd(2)–N(8)	171.08(15)	N(3)–Pd(2)–N(8)	95.48(15)	C(32)–N(7)–Pd(2)	114.7(3)
N(3)–Pd(2)–Pd(1)	65.03(11)	N(7)–Pd(2)–Pd(1)	111.76(11)	C(36)–N(7)–Pd(2)	125.4(3)
N3)–Pd(2)–N(1)	86.67(15)	C(42)–N(6)–Pd(1)	114.3(3)	C(27)–N(8)–Pd(2)	125.5(3)
N(3)–Pd(2)–N(8)	174.40(14)	C(46)–N(6)–Pd(1)	125.5(3)	C(31)–N(8)–Pd(2)	114.0(3)
Bond	Dist.	Bond	Dist.	Bond	Dist.
H(25B)–O(8)	2.570	H(40)–O(10)	2.589	H(34)–O(6)	2.745
H(37)–O(9)	2.461	H(27)–O(5)	2.745	H(33)–O(6)	3.004
H(13A)–O(10)	2.589	H(1A)–O(6)	2.919	H(21)–O(7)	2.438

2. 5 Catalytic activity test

To explore the catalyst activity of pyrazolate-based dipalladium corners with weak dinuclear Pd(II)··Pd(II) intramolecular bonding interaction, different reaction conditions have been tried to obtain the feasible solution.

In a typical experiment, the iodobenzene (204 mg, 1 mmol), benzeneboronic acid (182 mg, 1 mmol), K_3PO_4 (318.4 mg, 1.5 mmol) and dipalladium corners C1·$2NO_3^-$ (14 mg, 10 μmmol), or C2·$2NO_3^-$ (14 mg, 10 μmmol), or C3·$2NO_3^-$ (14 mg, 10 μmmol), or C4·$2NO_3^-$ (14 mg, 10 μmmol) were added into a 100 mL flask. 30 mL 1,4-dioxane was added and the suspension was stirred at 100 °C under nitrogen atmosphere. After work up (monitored the consumption of the starting iodobenzene by TLC), the mixture was cooled to room temperature. The mixture was directly filtered and afforded the product through column chromatograph eluting with hexane/ethyl acetate. As shown in Table 2, all of the reactions exhibited product biphenyl in good yields except for HL^1 and HL^2.

Table 2. Catalytic Activity of Complexes $[(Dmbpy)_2Pd_2(NO_3)_2](NO_3)_2$, $[(bpy)_2Pd_2(NO_3)_2](NO_3)_2$, C1 $2NO_3$, C2 $2NO_3$, C3 $2NO_3$ and C4 $2NO_3$

Entry	Catalyst	Co-catalyst	Solvent	T/°C	Time/h	Yield/%
1	$[(dmbpy)_2Pd_2(NO_3)_2](NO_3)_2$	K_3PO_4	1,4-dioxane	100	24	82.4
2	$[(bpy)_2Pd_2(NO_3)_2](NO_3)_2$	K_3PO_4	1,4-dioxane	100	24	80.0
3	HL^1	K_3PO_4	1,4-dioxane	100	24	No reaction
4	HL^2	K_3PO_4	1,4-dioxane	100	24	No reaction
5	C1·$2NO_3^-$	K_3PO_4	1,4-dioxane	100	24	94.1
6	C2·$2NO_3^-$	K_3PO_4	1,4-dioxane	100	24	96.1
7	C3·$2NO_3^-$	K_3PO_4	1,4-dioxane	100	24	86.3
8	C4·$2NO_3^-$	K_3PO_4	1,4-dioxane	100	24	88.5

3 RESULTS AND DISCUSSION

3. 1 Synthesis and characterization

The ^1H and ^{13}C NMR analyses of the products clearly confirmed the formation of a single species with high symmetry, and integration of the signals indicated a 1:1 ratio of dimetal motifs ($[(bpy)Pd]^{2+}$ to the pyrazolate anion L^{1-} in the corner C1·2NO_3^- (Fig. 1). Remarkably, the ^1H NMR signals corresponding to the coordinated bpy moiety present three doublets at 8.59, 8.39, 8.36 ppm and one triplet at 7.81 ppm, respectively. The signals at 7.04, 6.98 and 6.94 ppm are attributed to protons of Ph-H from the pyrazole ligand L^1. The signals at 3.87 and 3.36 ppm are ascribed to the methyl protons of the OCH_3 groups. Notably, the L^1-OCH_3 protons of the ligand in complex C1·2NO_3^- were split into two signals of 3.87 and 3.36 ppm, while the signal of CH_3 at 3.76 ppm before the reaction. The L^1-methyl protons of the ligand in the product were split into two signals of 2.52 and 2.33 ppm, while the signal of the CH_3 at 2.17 ppm before the reaction. In the FT-IR spectra, the absorption bands in the region of 3200~3500 cm^{-1} can be attributed to the stretching vibrations of O–H. The bands in the region of 2805~3010 cm^{-1} can be ascribed to the C–H stretching vibrations of benzene ring, and the absence of the absorption bands at 1450~1600 cm^{-1} to the C–C stretching vibrations of benzene ring. The formation of C1 is further supported by ESI-MS in Fig. 2. Two peaks at 493.1 and 1132.2 were corresponding to the $[C1]^{2+}$ and $[C1·PF_6^-]^+$ which confirmed C1 has a dimetal structure. The other three similar complexes C2, C3 and C4 were obtained and characterized by the same method (See SI for the synthesis).

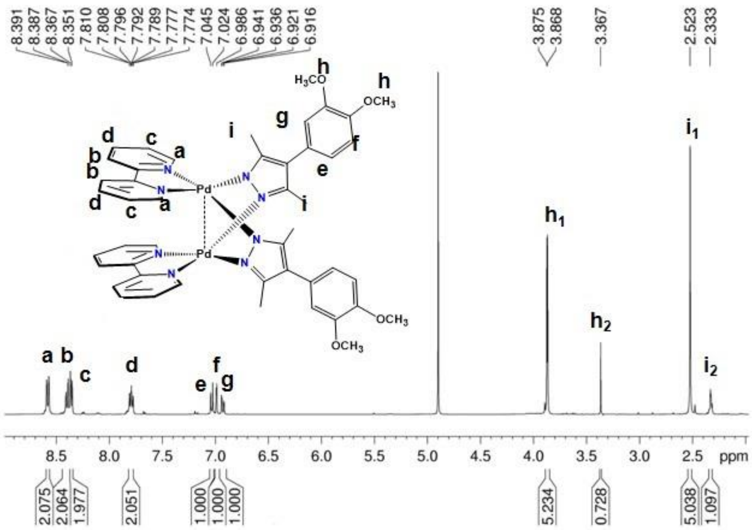

Fig. 1. **^1H NMR spectrum of C1·2NO_3^- at 298 K**

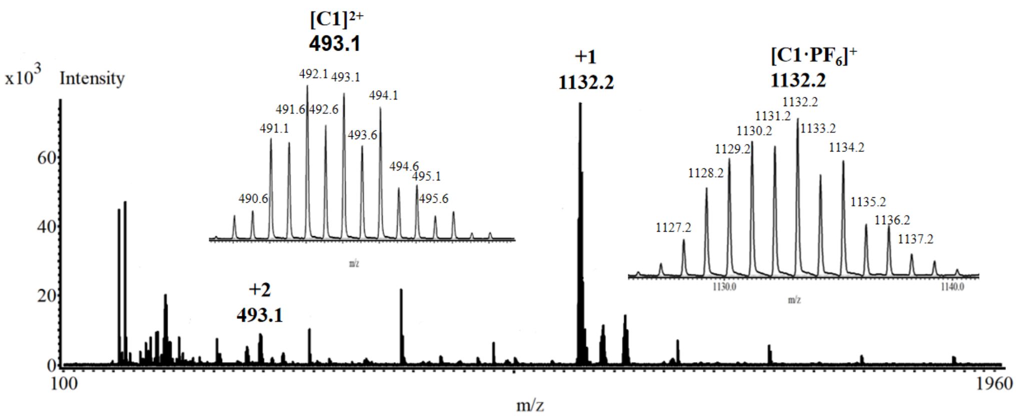

Fig. 2. **ESI-MS spectrum of C1·2PF_6^- in acetonitrile; the inset shows the isotopic distribution of the species $[C1·PF_6^-]^+$ and $[C1]^{2+}$**

All the characterizations have demonstrated that these molecular corners have been successfully prepared. The solid state structures of these "dimetallic corners" were further confirmed by single-crystal X-ray diffraction.

3. 2 X-ray crystal structure

The structure of complex $C1·2NO_3^-$ was successfully determined by X-ray diffraction as depicted in Fig. 3 (Further views and tables with bond lengths and angles are provided in Table 1). Single crystals of $C1·2NO_3^-$ were obtained by vapor diffusion isopropyl ether into their metanol solutions. $C1·2NO_3^-$ crystallizes in space group $P2_1/c$. The structure reveals a Pd2 dimetallic corner-shaped structure with difunctional ligands doubly bridged $[Pd(bpy)]_2$ dimetal corner. The $[Pd_2L_2]$-type corner is supported by two pyrazolate ligands and one $Pd_2(bpy)_2$ motif (Fig. 3a). The central six-membered ring consisting of two Pd(II) atoms and four pyrazole N atoms has a boat-shaped conformation with THE Pd-Npz distances falling between 1.99 and 2.01 Å. The Pd(1)–Pd(2) separation is 3.07 Å and the dihedral angle of two bpys in the corner is 43.72 °. The deprotonated ligands (L^1) are nearly perpendicular to each other with the dihedral angle being 99.08 °. And this arrangement creates an ''open book'' disposition for the square-planar environment of the two Pd atoms. As shown in Fig. 3b, dimetallic coordination corner can be stuck into a two-dimensional structure via strong multiple hydrogen bonding and weak *π*-*π* stacking interactions. As shown in Fig. 3c and 3d, nine intermolecular hydrogen bonds were formed between oxygen acceptors O(5), O(6), O(7), O(8), O(9) and O(10) from two nitrate anions and ligand H donors (H(1A), H(13A), H(21), H(25B), H(27), H(33), H(34), H(37) and H(40)). The distances of hydrogen bonds vary from 2.438 to 3.004 Å, as shown in Table 1. The distance of the phenyl and pyridyl rings in the next $C1·2NO_3^-$ is 4.014 Å, and they are nearly parallel to each other with their dihedral angle of 189.88 °, falling in the range of *π*-*π* interactions. Meanwhile, the phenyl rings in $C1·2NO_3^-$ are engaged in C–H ··*π* contacts with a centroid-to-plane distance of 3.805 Å.

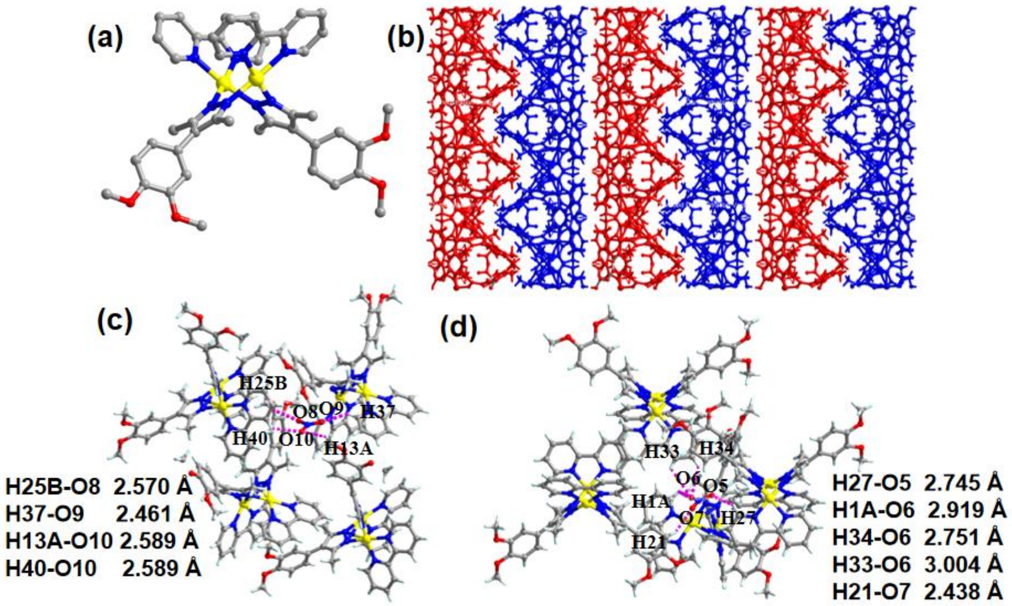

Fig. 3. Crystal structure of $C1·2NO_3^-$, top view (a), stacking mode (b), multiple hydrogen bond interaction modes between nitrate and ligands (c, d). (A) –1 + *x*, –0.5 – *y*, 0.5 + *z*; (B) –*x*, –0.5 + *y*, 0.5 – *z* (yellow: Pd; gray: C; light grey: H; blue: N; red: O)

3. 3 Catalytic activity

In this work, we introduce the OCH_3 and pyridine groups into the functional pyrazole-bridged metallo-corners to improve the solubility of metallo-corners $[Pd_2L_2]^{2+}$. As shown in Table 3 and Table S1, six different iodine-substituted and boronic acid-substituted aromatic compounds were chosen to react under similar conditions. In these cases, the desirable products were obtained in high yields, referring to the excellent catalytic activities of $C1·2NO_3^-$~$C4·2NO_3^-$. In addition, electron-donating (-OMe, -Me) boric acids tend to have higher yields than the electron-withdrawing groups (-CHO) boric acids during the reactions[29, 30]. However, no catalytic activity was observed upon using HL^1 and HL^2 alone. This remarkable difference in catalytic activity was attributed to the tunable impact and weak dinuclear Pd(II)··Pd(II) intramolecular bonding interaction of complexes $C1·2NO_3^-$ ~ $C4·2NO_3^-$.

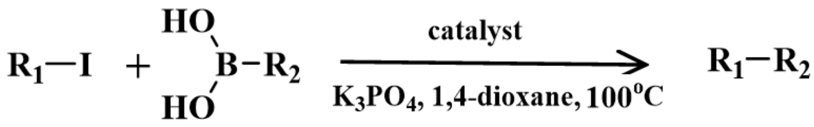

Table 3. Scope of Dimetal Complex C1·2NO_3^- Catalyst for Suzuki-coupling Reactions

Entry	Catalyst	R_1	R_2	Yield (%)
1	C1·2NO_3^-	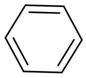	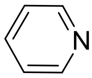	84.6
2	C1·2NO_3^-	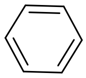	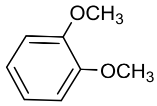	88.0
3	C1·2NO_3^-	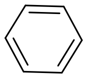	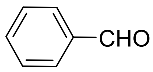	83.1
4	C1·2NO_3^-	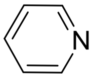	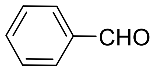	80.8
5	C1·2NO_3^-	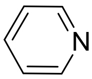	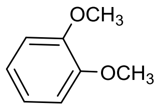	84.5
6	C1·2NO_3^-	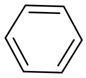	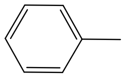	92.3

4 CONCLUSION

In conclusion, a series of novel positively-charged pyrazolate-bridged "molecular clips" C1·2NO_3^- ~ C4·2NO_3^- were successfully synthesized. The crystal structure of C1·2NO_3^- reveals a Pd_2 dimetallic clip-shaped structure, and the [Pd_2L_2]-type corner is supported by two ditopic pyrazolate-based ligands and Pd(II) ··Pd(II) dimetal-coordination motifs. Interestingly, a 2D supramolecular network has been constructed by clip-shaped coordination corners and two nitrate anions via multiple hydrogen bonds in the semi-open cavity. The clip-shaped metallo-corners were characterized by single-crystal X-ray diffraction analysis, ^{1}H and ^{13}C NMR, high resolution electrospray ionization mass spectrometry and elemental analysis. More interestingly, dipalladium clips C1·2NO_3^- ~ C4·2NO_3^- with weak Pd(II) ··Pd(II) intramolecular bonding interactions exhibit an excellent catalytical performance in Suzzki-coupling reaction.

REFERENCES

(1) Sauvage, J. P. *Transition Metals in Supramolecular Chemistry, Perspectives in Supramolecular Chemistry.* Vol. 5, Wiley, New York **1999**.

(2) Fujita, M. *Molecular Self-assembly Organic Versus Inorganic Approach (Structure and Bonding)*. Vol. 96, Springer, New York **2000**.

(3) Chakrabarty, R.; Mukherjee, P. S.; Stang, P. J. Supramolecular coordination: self-assembly of finite two- and three-dimensional ensembles. *Chem. Rev*. **2011**, 111, 6810–6918.

(4) Wang, W.; Wang, Y. X.; Yang, H. B. Supramolecular transformations within discrete coordination-driven supramolecular architectures. *Chem. Soc. Rev*. **2016**, 45, 2656–2693.

(5) Care, J. B. *Introduction to Ligand Field Theory*. New York: McGraw Hill **1962**.

(6) Brown, C. J.; Toste, F. D.; Bergman, R. G.; Raymond, K. N. Supramolecular catalysis in metal-ligand cluster hosts. *Chem. Rev*. **2015**, 115, 3012–3035.

(7) Xu, H.; Chen, R. F.; Sun, Q.; Lai, W. Y.; Su, Q. Q.; Huang, W.; Liu, X. G. Recent progress in metal-organic complexes for optoelectronic applications.

Chem. Soc. Rev. **2014**, 43, 3259–3302.

(8) Tiwari, V. K.; Mishra, B. B.; Mishra, K. B.; Mishra, N.;Singh, A.; Chen, X. Cu-catalyzed click reaction in carbohydrate chemistry. *Chem. Rev*. **2016**, 116, 3086–3240.

(9) Yu, S. Y.; Li, S. H.; Huang, H. P.; Zhang, Z. X.; Jiao, Q.; Shen, H.; Hu, X. X.; Huang, H. Molecular self-assembly with modularization and directionality: vectormanipulation at metal centers. *Curr. Org. Chem*. **2005**, 9, 555–563.

(10) Ismayilov, R. H.; Wang, W. Z.; Lee, G. H.; Yeh, C. Y.; Hua, S. A.; Song, Y.; Rohmer, M. M.; Bénard, M.; Peng, S. M. Two linear undecanickel mixed-valence complexes: increasing the size and the scope of the electronic properties of nickel metal strings. *Angew. Chem. Int. Ed*. **2011**, 50, 2045–2048.

(11) Mitsumi, M.; Ueda, H.; Furukawa, K.; Ozawa, Y.; Toriumi, K.; Kurmoo, M. Constructing highly conducting metal-metal bonded solids by electrocrystallization of $[Pt^{II}_2(RCS_2)_4]$ (RCS_2^- = dithiocarboxylato, R = methyl or ethyl). *J. Am. Chem. Soc*. **2008**, 130, 14102–14104.

(12) Qin, J. H.; Huang, Y. D.; Shi, M. Y.; Wang, H. R.; Han, M. L.; Yang, X. G.; Li, F. F.; Ma, L. F. Aqueous-phase detection of antibiotics and nitroaromatic explosives by an alkali-resistant Zn-MOF directed by anionic liquid. *RSC Adv*. **2020**, 10, 1439–1446.

(13) Yam, V. W. W.; Au, V. K. M.; Leung, S. Y. L. Light-emitting self-assembled materials based on d^8 and d^{10} transition metal complexes. *Chem. Rev*. **2015**, 115, 7589–7728.

(14) Marques, A. J.; Palanimurugan, R.; Matias, A. C.; Ramos, P. C.; Dohme, R. J. Catalytic mechanism and assembly of the proteasom. *Chem. Rev*. **2009**, 109, 1509–1536.

(15) Park, J.; Hong, S. Cooperative bimetallic catalysis in asymmetric transformations. *Chem. Soc. Rev*. **2012**, 41, 6931–6943.

(16) Qin, J. H.; Huang, Y. D.; Zhao, Y.; Yang, X. G.; Li, F. F.; Wang, C.; Ma, L. F. Highly dense packing of chromophoric linkers achievable in a pyrene-based metal-organic framework for photoelectric response. *Inorg. Chem*. **2019**, 58, 15013–15016.

(17) Friis, S. D.; Pirnot, M. T.; Dupuis, L. N.; Buchwald, S. L. A dual palladium and copper hydride catalyzed approach for alkyl-alkyl cross-coupling of aryl halides and olefins. *Angew. Chem. Int. Ed*. **2017**, 56, 7242–7724.

(18) Zhang, J. J.; Hu, S. M.; Xiang, S. C.; Sheng, T.; Wu, X. T.; Li, Y. M. Syntheses, structures, and properties of high-nuclear 3*d*-4*f* clusters with amino acid as ligand: $\{Gd_6Cu_{24}\}$, $\{Tb_6Cu_{26}\}$, and $\{(Ln_6Cu_{24})_2Cu\}$ (Ln = Sm, Gd). *Inorg. Chem*. **2006**, 45, 7173–7181.

(19) Yu, S. Y.; Lu, H. L. From metal-metal bonding to supra-metal-metal bonding directed self-assembly: supramolecular architectures of group 10 and 11 metals with ligands from mono- to poly-pyrazoles. *Isr. J. Chem*. **2019**, 59, 166–183.

(20) Halcrow, M. A. Pyrazoles and pyrazolides-flexible synthons in self-assembly. *Dalton Trans*. **2009**, 2059–2073.

(21) Chen, H.; Yu, Z. C.; Deng, W.; Jiang, X. F.; Yu, S. Y. Pyrazolate-based dipalladium (II, II) complexes: synthesis, characterization and catalytical performance in Suzuki-coupling reaction. *Chin. J. Inorg. Chem*. **2017**, 33, 939–946.

(22) Qin, L.; Yao, L. Y.; Yu, S. Y. Self-assembly of $[M_8L_4]$ and $[M_4L_2]$ fluorescent metallo macrocycles with carbazole-based dipyrazole ligands. *Inorg. Chem*. **2012**, 51, 2443–2453.

(23) Hu, Z. Y.; Deng, W.; Lu, H. L.; Huang, H. P.; Yu, S. Y. Mononuclear assemblies with metal-metal interaction: syntheses and catalytical performance in Suzuki-coupling reaction. *Chin. J. Inorg. Chem*. **2018**, 34, 387–396.

(24) Brown, C. J.; Toste, F. D.; Bergman, R. G.; Raymond, K. N. Supramolecular catalysis in metal-ligand cluster hosts. *Chem. Rev*. **2015**, 115, 3012–3035.

(25) Sun, W. Q.; Tong, J.; Lu, H. L.; Ma, T. T.; Ma, H. W.; Yu, S. Y. Programmable self-assembly of heterometallic palladium(II)-copper(II) 1D grid-chain using dinuclear palladium(II) corners with pyrazole-carboxylic acid ligands. *Chem. Asian J*. **2018**, 13, 1108–1113.

(26) Hu, Z. Y.; Deng, W.; Lu, H. L.; Huang, H. P.; Yu, S. Y. Mononuclear assemblies with metal-metal interaction: syntheses and catalytical performance in suzuki-coupling reaction. *Chin. J. Inorg. Chem*. **2015**, 31, 1278–1286.

(27) Sheldrick, G. M. *SHELXS-97, Program for the Solution of Crystal Structure*. University of Göttingen, Germany **1997**.

(28) Sheldrick, G. M. *SHELXL-97, Program for the Refinement of Crystal Structure*. University of Göttingen, Germany **1997**.

(29) Reek, J. N. H.; Arevalo, S.; Heerbeek, R. V.; Kamer, P. C. J.; Leeuwen, P. V. *Advances in Catalysis*, Vol 49, Academic Press, Amsterdam **2006**, 71–151.

(30) Brown, H. C. *Organic Syntheses via Boranes*. Wiley, New York **2001**.